

# Direct assembly of nanowires by electron beam-induced dielectrophoresis

**Chang, Bingdong; Zhao, Ding**

*Published in:*
Nanotechnology

*Link to article, DOI:*
10.1088/1361-6528/abeeb5

*Publication date:*
2021

*Document Version*
Peer reviewed version

# Direct assembly of nanowires by electron beam-induced dielectrophoresis

*Bingdong Chang* [1] *

bincha@dtu.dk

*Ding Zhao* [2, 3] *

zhaoding@westlake.edu.cn

[1] DTU Nanolab, Technical University of Denmark, Ørsteds Plads, Building 347, 2800 Kgs. Lyngby, Denmark.

[2] Key Laboratory of 3D Micro/Nano Fabrication and Characterization of Zhejiang Province, School of Engineering, Westlake University, Hangzhou 310024, China

[3] Institute of Advanced Technology, Westlake Institute for Advanced Study, Hangzhou 310024, China

KEYWORDS

Self-assembly, dielectrophoresis, dielectrophoretic force, electron beam, 3D nanostructures,

ABSTRACT

Controllable self-assembly is an important tool to investigate interactions between nanoscale objects. Here we present an assembly strategy based on 3D aligned silicon nanowires. By illuminating the tips of nanowires locally by a focused electron beam, an attractive dielectrophoretic force can be induced, leading to elastic deformations and sticking between adjacent nanowires. The whole process is performed feasibly inside a vacuum environment free from capillary or hydrodynamic forces. Assembly mechanisms are discussed for nanowires in both one and two layers, and various ordered organizations are presented. With the help of moisture treatment, a hierarchical assembly can also be achieved. Notably, an unsynchronized assembly is observed in two layers of nanowires. This study helps with a better understanding of nanoscale sticking phenomena and electrostatic actuations in nanoelectromechanical systems, besides, it also provides possibilities to probe quantum effects like Casimir forces and phonon heat transport in a vacuum gap.

## 1. INTRODUCTION

Self-assembly has been an attractive field in micro- and nanoscale science and engineering. [1 - 3] By employing building blocks like chemically synthesized nanoparticles [4] or top-bottom fabricated nanostructures, [5, 6] a long-range spatial order can be achieved for practical applications such as particle trapping, surface-enhanced Raman spectroscopy [7] and optical metasurfaces. [8] As the dimension of assembly units continues shrinking down towards nanoscale or even molecular levels, the self-assembly dynamics will be dominated by forces which are otherwise negligible in

macroscopic objects, e. g. capillary force, van der Waals force and Casimir force. They are often utilized to actuate self-assembly processes, and in the same time offering opportunities to probe interaction mechanisms between nanoscale objects.

Dielectrophoresis is an interesting phenomenon where a dielectric nanostructure will experience a force when placed inside a non-uniform electric field, with medium possessing a different permittivity. The dielectrophoretic (DEP) force can be either attractive or repulsive depending on the geometry and material properties. [9] Hence, particle manipulation and large-scale assembly become feasible based on this effect. By designing pairs of electrodes, [10, 11] or simply applying a charged metallic tip, [12] silicon nanowires (SiNWs) or nanoparticles can be controlled intentionally in electrolytes or vacuum environments, leading to deterministic organizations of assembly units. Different from nanoparticles, which are intrinsically isotropic in assembly processes, nanowires are susceptible to external forces in an anisotropic manner, thus can lead to more complex physical phenomena. Taking advantages of the elasticity of nanowires in transverse directions, complex assembly patterns has been demonstrated to mimic biological systems in natural scenarios.[13]

In this study, we present an alternative self-assembly of 3D aligned SiNW arrays, which is based on elastic deformation of SiNWs actuated locally by a focused electron-beam (e-beam). The e-beam is generated conveniently from a scanning electron microscope (SEM) and the whole assembly process occurs inside a vacuum environment free from electrolytes or ambient air. During the process, a divergent electric field is generated at the tip of the irradiated nanowire, which will then induce dipole moments in the adjacent nanowires. Finally, attractive DEP forces will trigger a cascade of sticking events along the nanowire arrays. The width of each SiNW is around 50 nm, and a long-range order up to 15 μm can be achieved with various regular morphologies. This study provides a unique perspective on nanoscale self-assembly processes, and

in the same time opens up new possibilities to probe the interactions inside nanomechanical systems.

## 2. RESULTS AND DISCUSSIONS

Figure 1a illustrates schematically the fabrication process of 3D aligned SiNW arrays. Resist patterns were first defined by e-beam lithography, afterwards a modified plasma etching process was performed to sculpture 3D nanowires, which are aligned horizontally compared to the wafer surface. Details on this 3D fabrication technique have been introduced in our previous studies. [14 - 16] The fabricated nanowires have a height of 80 nm and width of 50 nm, and the length can vary from 500 nm to 2.5 μm, corresponding to an aspect ratio up to 50, which can be difficult to achieve with standard top-down fabrication processes. We remove the e-beam resist by plasma ashing, and then transfer the samples immediately into an SEM. A focused e-beam is employed to illuminate at the tips of SiNWs (Figure 1b). It should be noticed that the incident electrons not only serve as a source for the inspection of nanostructures, but also induce charges at the nanowire tips. The distribution of generated electric field around the SiNWs is qualitatively displayed in Figure 1c, where simulations were performed by solving Poisson's equations with a finite difference method. Due to the limited electron mobility of silicon and the high aspect ratio of suspended nanowires, the charges from incident electrons can be considered as well confined at the end of SiNWs, while the bulk substrate is grounded with a zero potential. Since adjacent nanowires are not being illuminated, they are consequently placed inside a non-uniform electric field, which drives the dynamic assembly processes.

To demonstrate the morphology of 3D SiNW arrays, we fabricated various layers of suspended SiNWs with both ends fixed onto the substrate (Figure 1d). The wiggling geometry is often observed for plasma-etched nanostructures, especially with fine features below 50 nm. This is

assumed to be caused by ion-induced stress inside the resist mask layer. [17, 18] However, during the assembly process to be discussed below, the mask layer is removed and only one side of the nanowire is attached to the bulk substrate, thus the residual stress can be released. Compared with traditional SiNW structures, which are normally etched or synthesized vertically to wafer surface, this type of horizontally aligned SiNWs have shown special potentials in nanophotonics [19, 20] and nanoelectronics. [21, 22]

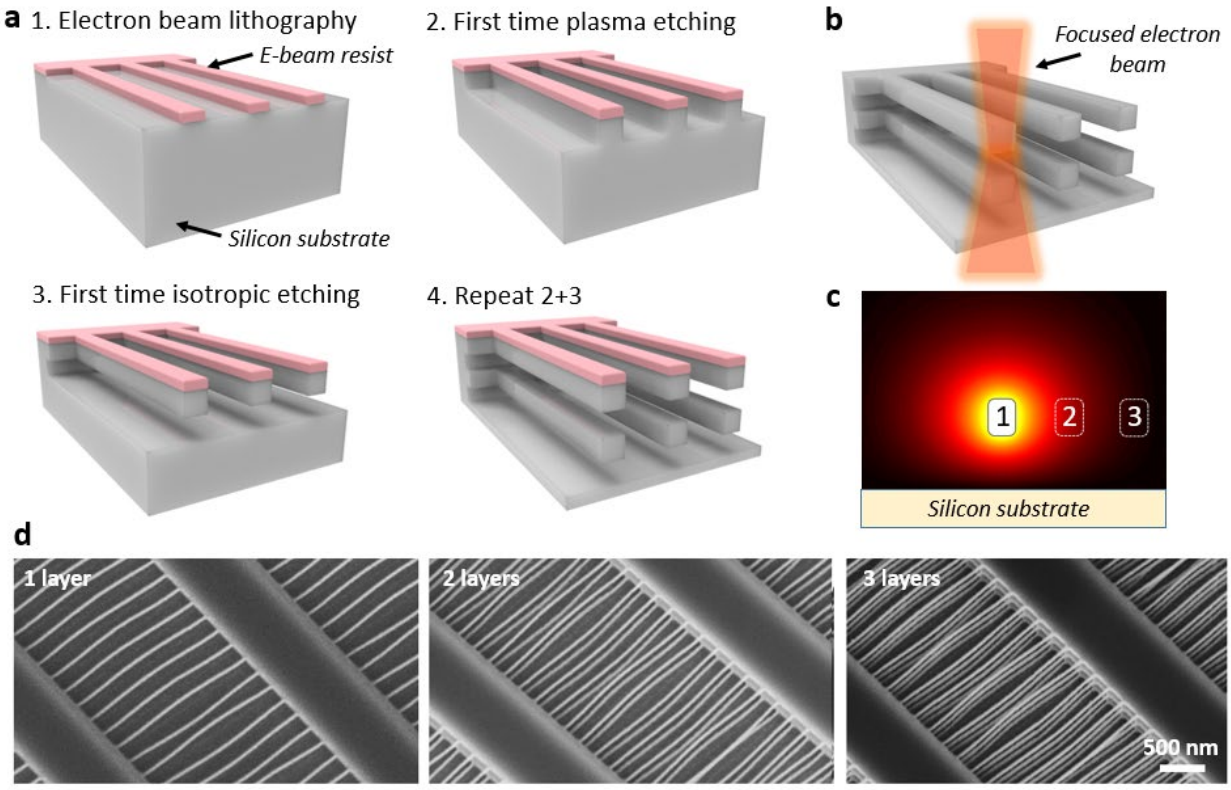


**Figure 1.** (a) Process flow for fabrication of 3D aligned SiNWs; (b) Schematic illustration showing how self-assembly can be triggered by a focused electron beam; (c) Simulated distribution of electric field intensity from a cross-section view, showing the divergent electric field generated by the charged nanowire (labeled as 1); (d) SEM images of fabricated 3D multilayer SiNW arrays.

We start first with the discussion of assembly mechanisms for a single layer of SiNWs. As shown in figure 2a, SiNW 1 is illuminated by the e-beam and charged negatively. An electric field gradient is generated across SiNW 2 by the divergent field, resulting in a new charge equilibrium inside SiNW 2. As the permittivity of silicon is higher than the vacuum environment, the bound charges will lead to a dipole moment across SiNW 2, which is aligned with electric field lines between SiNW 1 and 2. A DEP force $F_{dep}$ is exerted on the tip of SiNW 2 towards SiNW 1, and the magnitude of the translational force can be written as: [23]

$$\langle F_{DEP} \rangle = \frac{hw\Delta l}{4} Re[\alpha] \nabla |E|^2 \propto \frac{hw\Delta l}{d^3} \quad (1)$$

Here $h$ and $w$ are the height and width of an individual nanowire, $d$ is the distance between two adjacent nanowires. $E$ represents the local electric field, and $\Delta l$ is the length of the irradiated segment on nanowires. The effective polarizability of dipole moment at SiNW 2 is labeled as $\alpha$, since the electric field is frequency-independent, we can rewrite it as $\alpha = 3(\varepsilon_{Si} - 1)/(\varepsilon_{Si} + 2)$, in which $\varepsilon_{Si}$ is the relative permittivity of silicon (around 11.68 in normal condition). As the effective polarizability $\alpha > 0$, the induced DEP force is attractive and drives SiNW 2 towards 1.

For an array of SiNWs labeled as $i$, $j$, $k$ and $l$ (Figure 2b), we first illuminate SiNW $i$ (in red color) at its tip. SiNW $j$ will be attracted by a DEP force $F_{ji}$ towards $i$, which leads to elastic deformations of both nanowires and pulls $j$ closer to $i$. It should be mentioned that $j$ will also experience an attractive DEP force $F_{jk}$ towards $k$, which is induced by redistributed charges on $k$. However, the distance between $j$ and $i$ is smaller compared with the distance between $j$ and $k$. According to equation (1), $\langle F_{DEP} \rangle \propto 1/d^3$, the DEP forces satisfy $|F_{ji}| > |F_{jk}|$. Hence, $j$ attaches to $i$ rather than $k$ and gets stuck by van der Waals force. When the e-beam scans further towards right, $k$ and $l$ will

also stick together by the induced DEP force $F_{kl}$ as $|F_{kl}| > |F_{kj}|$. In the end, all the SiNWs will be assembled by pairs along the e-beam scanning direction (see supplementary video). By designing the repeating unit of SiNW arrays, we obtain various ordered assembly structures in Figure 2c.

In order to make two adjacent nanowires bend and stick together, the DEP force should overcome the bending stiffness of nanowires. Following the classic Euler-Bernoulli beam theory, a bending force $F_B$ applied on the tip of SiNWs can be written as:

$$F_B = \frac{Ydw^3h}{8l^3} \propto \frac{dw^3h}{l^3} \quad (2)$$

In which $Y$ is the Young's modulus of silicon material, and the lateral displacement is calculated as half of the distance between adjacent nanowires. Since $F_B \propto w^3$, the nanowires with width of 80 nm are less bendable compared to narrower ones with width of 50 nm, which can be clearly seen in Figure 2c. In the case that $w$ = 50 nm, $h$ = 80 nm, $l$ = 2 μm and $d$ = 150 nm, the minimum bending force is calculated to be 3.75 nN. As the length of SiNWs is below the persistence length (~ 370 μm at room temperature), the influence of thermal fluctuations on the deformation of nanowires is negligible. [3] By approximating the contact of nanowire tips as a cylinder-cylinder interaction, the Van der Waals force can be estimated as $F_{VdW} = \frac{1}{16}Ah\sqrt{w/2}d_0^{-5/2} \approx 121\,nN$, which is significantly larger compared with the required bending force, implying that the assembled structures are mechanically robust. Here $d_0$ = 0.25 nm corresponding to the thickness of a monolayer of water molecules, [12] and we take the Hamaker constant A as $7.59 \times 10^{-20}\,J$. [24] It should be addressed that the bulk substrate is grounded to the sample holder, and $h$ is larger than $w$, giving a larger bending moment of inertia in the vertical direction, thus the nanowires are less likely to bend towards the substrate.

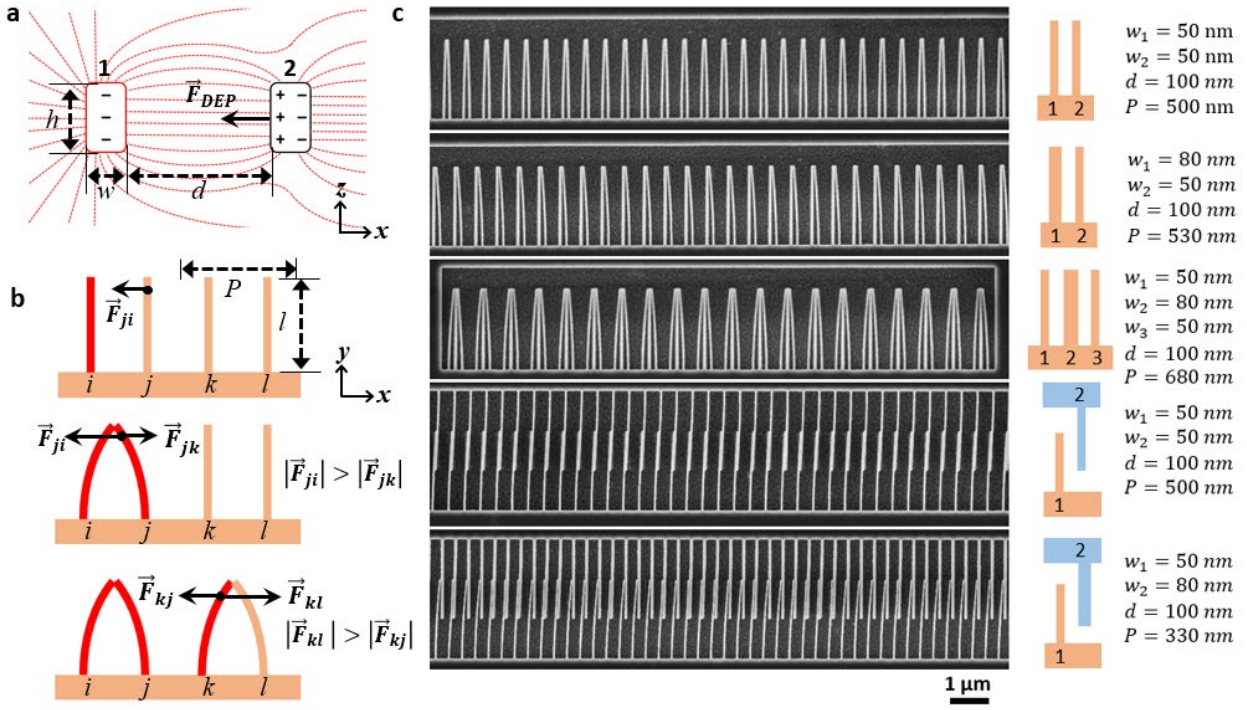


**Figure 2.** Direct self-assembly of 3D SiNW arrays in a single layer. (a) Schematic drawing of electric field distribution from a cross- section view, where SiNW 1 is illuminated by the e-beam and an attractive DEP force is induced on SiNW 2; (b) Schematic illustration from a top view, showing the dynamic assembly process for SiNW arrays (from top to bottom); (c) SEM images and corresponding parameters of repeating units for various SiNW arrays. Nanowires fixed on opposite sides are labeled in different colors.

We can see that the assembly process only happens, when the DEP force is larger than the minimum bending force, thus a simple analysis can be performed combining equation (1) and (2). As $|F_{DEP}| > |F_B|$ is required, a minimum length $l_{min}$ of SiNWs should exist for triggering the

assembly process. This criterion is verified by comparing the assembly yields of nanowire arrays with different $d$ and $l$ values (Figure 3a), which is shown in Figure 3a. To achieve over 80% yield, the minimum length $l_{min}$ of SiNWs should exceed 1.1 μm, 1.4 μm and 2 μm when the distance $d$ are 50 nm, 100 nm and 150 nm correspondingly. It indicates that $l_{min}$ increases with the distance between two adjacent nanowires. Another interesting phenomenon to be addressed is the cold welding-like coalescence of assembled nanowires. Figure 3b shows a pair of SiNWs with a point contact at the tip after e-beam irradiation. However, after moisture treatment, the gap between the nanowires is bridged by condensed water vapor and a line contact forms almost along the whole nanowires. This result is consistent with the capillary condensation reported in previous studies, where bundles of SiNWs can be assembled in large areas, [25] and the electrical resistance can be reduced between the junctions for applications like transparent conducting films. [26, 27] Furthermore, ordered hierarchical structures can be achieved by combining the moisture treatment with e-beam-induced assembly process. As illustrated in figure 3c, nanowire pairs are firstly assembled in SEM. After moisture treatment, nanowire pairs are coalesced by a line contact ($i$ and $j$, $k$ and $l$). It should be mentioned that the transition from the point contact to the line contact is supposed to be driven by capillary condensations, where the capillary forces at the meniscus are pulling the adjacent nanowires into each other. Then we illuminate the samples again with e-beams and the tip of coalesced nanowire pair ($i$ and $j$) attach to the adjacent nanowire pair ($k$ and $l$), leading to a higher assembly order. Experimental results are demonstrated in figure 3d and e. The former shows nanowire pairs isolate from each other with $P$ = 500 nm, while the later shows dense nanowire arrays with $P$ = 200 nm (Figure S1). Though this type of hierarchical assembly has been reported in a capillary-assisted assembly system, [5, 6] a liquid environment can be avoided in our strategy.

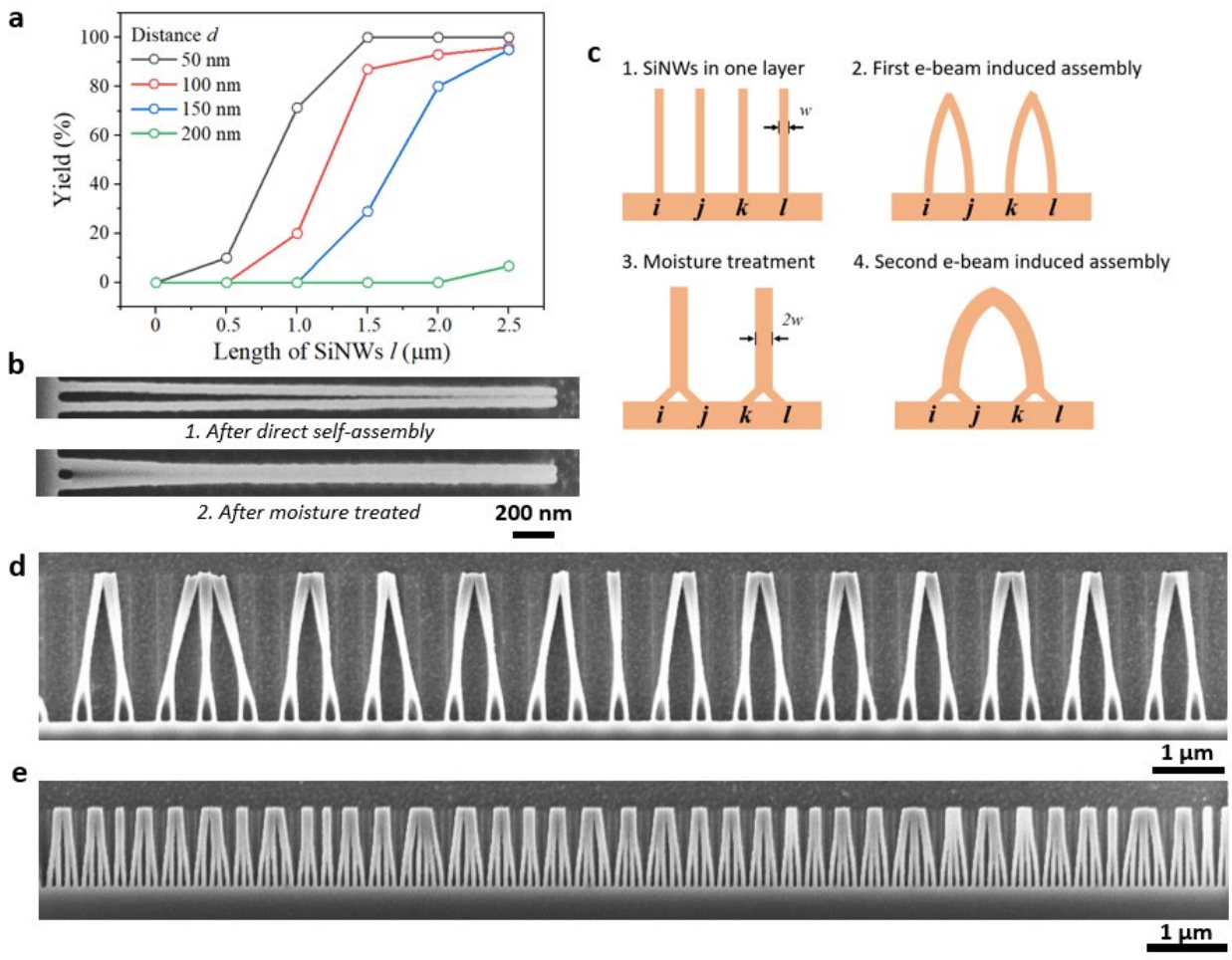


**Figure 3.** (a) Assembly yield in a single layer of SiNWs as a function of nanowire length and distance between adjacent nanowires; (b) Nanowire coalescence observed due to capillary condensation after the moisture treatment. Top: SEM image of an assembled nanowire pair; Bottom: SEM image of an assembled nanowire pairs after moisture treatment. (c) Schematic drawing of hierarchical assembly assisted by moisture treatment; (d) and (e) Hierarchical assembly of nanowire arrays with different periods.

Different from a single layer of nanowires, interactions in the vertical direction *z*-direction has to be taken into account for two layers of SiNWs. Figure 4a shows a schematic drawing, in which *i*, *j*, *k* are SiNWs on the top layer and *i'*, *j'* and *k'* are on the bottom layer. These two layers are

separated by a gap with the size $g \sim 80$ nm. Both *j* and *j'* are illuminated by the incident e-beam and negatively charged simultaneously (labeled in red color), which will then leads directly to electrostatic repulsive forces between *j* and *j'*. Since the bending moment of inertia of SiNWs in *z*-direction is around 2.5 times larger than in *x*-direction, the elastic displacement happens more easily in *x*-direction driven by the horizontal component of electrostatic forces, and *j* and *j'* bend in opposite directions along *x*-axis. Assuming the tip of *j* has a lateral displacement towards *i*, the induced DEP force $|F_{ij}|$ will overwin $|F_{kj}|$, as $\langle F_{DEP} \rangle \propto 1/d^3$. Similarly, the DEP forces on the bottom layer satisfy $|F_{i'j'}| < |F_{k'j'}|$. This asymmetric DEP force distribution breaks the synchronization of assembly processes between two layers, consequently *j* sticks to *i* while *j'* is paired with *k'*. As a proof of assembly mechanism, we fabricate two different configurations of nanowires with one end fixed on the same or opposite sides (more details in supplementary Figure S2). SEM images in figure 4b and c show clearly assembled SiNWs in two layers, where the top layer is labeled in red color and the bottom in blue. This well-defined assembly can also be achieved on a long-range order, exemplified by assembled SiNWs in two layers with a range over 15 μm in *x*-direction (Figure 4d). The irregularity on the right side is due to the termination of periodicity on the boundary.

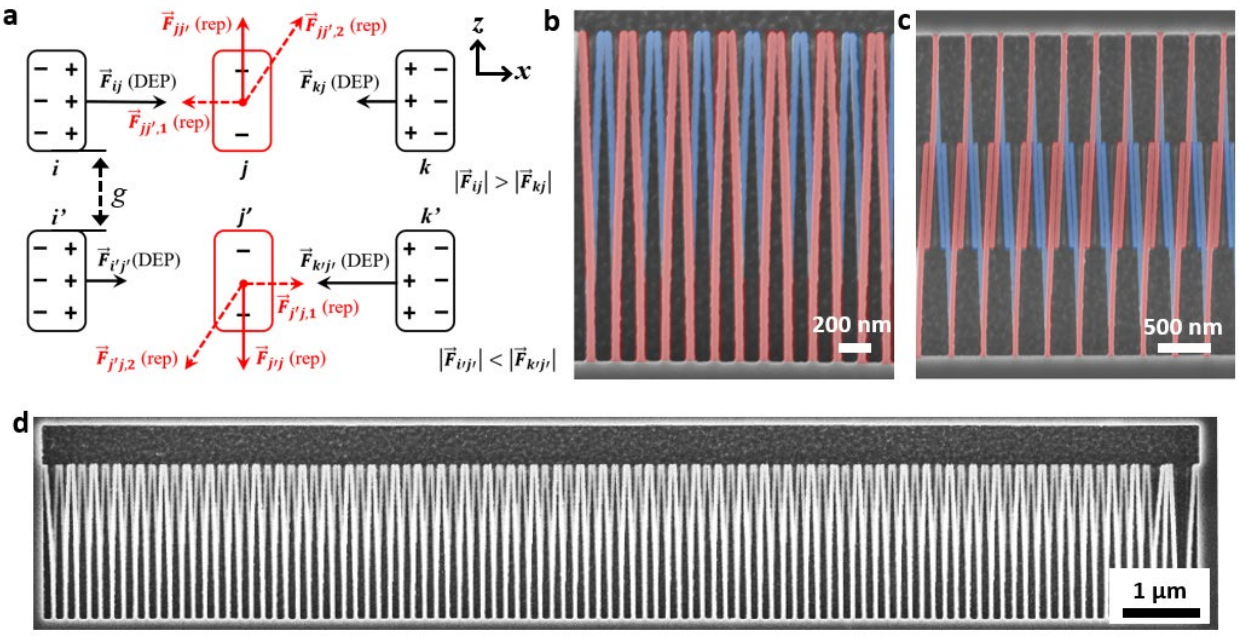


**Figure 4.** Direct self-assembly of 3D SiNW arrays in two layers. (a) Schematic diagram of assembly mechanism in two layers; SEM images of assembled nanowire arrays with one end fixed on (b) the same side or (c) opposite sides; (c) SEM image of assembled nanowires over a large area.

## 3. CONCLUSION

In conclusion, we introduce an assembly mechanism in nanoscale based on e-beam-induced dielectrophoresis. The assembling units are 3D aligned SiNWs with a width of around 50 nm and an aspect ratio up to 50. The elastic deformation of nanowires is actuated locally by an attractive DEP force, leading to a cascade of sticking events along the nanowire arrays. An ordered organization of assembled SiNWs in both one and two layers have been demonstrated. A capillary coalescence between pairs of assembled nanowires has been also observed. The whole assembly process occurs inside a vacuum environment free from liquids or gases, thus ruling out capillary forces and hydrodynamic forces, which are otherwise dominant in the assembly dynamics. Our

findings are beneficial to better understanding sticking phenomena [28] and electrostatic actuations in micro- and nanoelectromechanical systems. [29] Besides, our strategy opens up new possibilities to study the nanoscale interaction mechanism in electromechanical systems, where the scaled-down dimensions can give rise to various intriguing effects like Casimir force [30, 31] and photon heart transfer. [32]

## 4. METHODS

Electron beam lithography: patterning was performed with e-beam writer (Jeol JBX-9500FS, JEOL). The resist was positive-tone AR-P 649. 04 (Allresist GmbH) with a thickness of around 100nm. Acceleration voltage for e-beam exposure was 100 kV and the beam current was 10 nA. The critical dose in this condition was around 200 $\mu C/cm^2$.

3D plasma etching process: 3D SiNWs structures were fabricated with an inductively coupled plasma (ICP) etching system (DRIE Pegasus, SPTS). After etching, the e-beam resist was removed from sample surfaces by oxygen plasma inside a plasma asher system (TePla 300, PVA TePla).

Assembly process: self-assembly was performed inside a SEM system (SEM Supra 60VP, Carl Zeiss AG). Incident e-beam was focused on the tip of individual SiNW in sequence. An acceleration voltage of 5 kV was chosen, with the aperture size of 20 μm and chamber pressure of $5\times10^{-6}$ mbar. Assembly can be observed with acceleration voltages between 1 kV and 20 kV. In order to achieve a balance between imaging quality and assembly efficiency, the acceleration voltage and the aperture size are chosen to 5 kV and 20 μm, respectively. The incident electrons are focused at the tip of the SiNWs, which can reduce the critical dielectrophoretic force for nanowire deformations and thus a higher assembly efficiency. Moisture was applied by simply breathing on to the sample surface, afterwards baked out on a hotplate with temperature of 200 °C.

ASSOCIATED CONTENT

**Supporting Information**. The following files are available free of charge.

Video recording the assembly process with a single layer of nanowires (mp4)

SEM images showing the details of assembled nanowires (PDF)

AUTHOR INFORMATION

**Corresponding Author**

Email: bincha@dtu.dk; zhaoding@westlake.edu.cn

**Funding Sources**

This work was supported by VILLUM FONDEN (No. 00027987). D. Z. acknowledges the support from the National Natural Science Foundation of China (61927820) and the China Postdoctoral Science Foundation (2020M671810, 2020T130602).

ACKNOWLEDGMENT

We thank the DTU Nanolab staff for instrument support.

REFERENCES

[1] Nie, Z., Petukhova, A., & Kumacheva, E. (2010). Properties and emerging applications of self-assembled structures made from inorganic nanoparticles. Nature nanotechnology, 5(1), 15-25.

[2] Ong, L. L., Hanikel, N., Yaghi, O. K., Grun, C., Strauss, M. T., Bron, P., ... & Kishi, J. Y. (2017). Programmable self-assembly of three-dimensional nanostructures from 10,000 unique components. Nature, 552(7683), 72-77.

[3] Cohen, A. E., & Mahadevan, L. (2003). Kinks, rings, and rackets in filamentous structures. Proceedings of the National Academy of Sciences, 100(21), 12141-12146.

[4] Ni, S., Leemann, J., Buttinoni, I., Isa, L., & Wolf, H. (2016). Programmable colloidal molecules from sequential capillarity-assisted particle assembly. Science advances, 2(4), e1501779.

[5] Pokroy, B., Kang, S. H., Mahadevan, L., & Aizenberg, J. (2009). Self-organization of a mesoscale bristle into ordered, hierarchical helical assemblies. Science, 323(5911), 237-240.

[6] Duan, H., & Berggren, K. K. (2010). Directed self-assembly at the 10 nm scale by using capillary force-induced nanocohesion. Nano letters, 10(9), 3710-3716.

[7] Liberman, V., Yilmaz, C., Bloomstein, T. M., Somu, S., Echegoyen, Y., Busnaina, A., ... & Rothschild, M. (2010). A nanoparticle convective directed assembly process for the fabrication of periodic surface enhanced Raman spectroscopy substrates. Advanced Materials, 22(38), 4298-4302.

[8] Gupta, T. D., Martin-Monier, L., Yan, W., Le Bris, A., Nguyen-Dang, T., Page, A. G., ... & Sorin, F. (2019). Self-assembly of nanostructured glass metasurfaces via templated fluid instabilities. Nature nanotechnology, 14(4), 320-327.

[9] Pohl, H. A. (1958). Some effects of nonuniform fields on dielectrics. Journal of Applied Physics, 29(8), 1182-1188.

[10] Freer, E. M., Grachev, O., Duan, X., Martin, S., & Stumbo, D. P. (2010). High-yield self-limiting single-nanowire assembly with dielectrophoresis. Nature nanotechnology, 5(7), 525.

[11] Raychaudhuri, S., Dayeh, S. A., Wang, D., & Yu, E. T. (2009). Precise semiconductor nanowire placement through dielectrophoresis. Nano letters, 9(6), 2260-2266.

[12] Denisyuk, A. I., Komissarenko, F. E., & Mukhin, I. S. (2014). Electrostatic pick-and-place micro/nanomanipulation under the electron beam. Microelectronic engineering, 121, 15-18.

[13] Bico, J., Roman, B., Moulin, L., & Boudaoud, A. (2004). Elastocapillary coalescence in wet hair. Nature, 432(7018), 690-690.

[14] Chang, B., Jensen, F., Hübner, J., & Jansen, H. (2018). DREM2: a facile fabrication strategy for freestanding three dimensional silicon micro-and nanostructures by a modified Bosch etch process. Journal of Micromechanics and Microengineering, 28(10), 105012.

[15] Chang, B., Zhou, C., Tarekegne, A. T., Yang, Y., Zhao, D., Jensen, F., ... & Jansen, H. (2019). Large Area Three‐Dimensional Photonic Crystal Membranes: Single‐Run Fabrication and Applications with Embedded Planar Defects. Advanced Optical Materials, 7(2), 1801176.

[16] Chang, B., Tang, Y., Liang, M., Jansen, H., Jensen, F., Wang, B., ... & Sun, H. (2019). Highly ordered 3D silicon micro‐mesh structures integrated with nanowire arrays: A multifunctional platform for Photodegradation, photocurrent generation, and materials conversion. ChemNanoMat, 5(1), 92-100.

[17] Darnon, M., Chevolleau, T., Joubert, O., Maitrejean, S., Barbe, J. C., & Torres, J. (2007). Undulation of sub-100 nm porous dielectric structures: A mechanical analysis. Applied Physics Letters, 91(19), 194103.

[18] Stan, G., Ciobanu, C. V., Levin, I., Yoo, H. J., Myers, A., Singh, K., ... & King, S. W. (2015). Nanoscale buckling of ultrathin low-k dielectric lines during hard-mask patterning. Nano Letters, 15(6), 3845-3850.

[19] Cao, L., Fan, P., & Brongersma, M. L. (2011). Optical coupling of deep-subwavelength semiconductor nanowires. Nano letters, 11(4), 1463-1468.

[20] Yi, S., Zhou, M., Yu, Z., Fan, P., Behdad, N., Lin, D., ... & Brongersma, M. (2018). Subwavelength angle-sensing photodetectors inspired by directional hearing in small animals. Nature nanotechnology, 13(12), 1143-1147.

[21] Lee, B. H., Hur, J., Kang, M. H., Bang, T., Ahn, D. C., Lee, D., ... & Choi, Y. K. (2016). A vertically integrated junctionless nanowire transistor. Nano letters, 16(3), 1840-1847.

[22] Lee, B. H., Ahn, D. C., Kang, M. H., Jeon, S. B., & Choi, Y. K. (2016). Vertically integrated nanowire-based unified memory. Nano letters, 16(9), 5909-5916.

[23] Jones, T. B. (1979). Dielectrophoretic force calculation. Journal of Electrostatics, 6(1), 69-82.

[24] Bergström, L. (1997). Hamaker constants of inorganic materials. Advances in colloid and interface science, 70, 125-169.

[25] Zhao, Y. P., & Fan, J. G. (2006). Clusters of bundled nanorods in nanocarpet effect. Applied physics letters, 88(10), 103123.

[26] Lu, H., Zhang, D., Cheng, J., Liu, J., Mao, J., & Choy, W. C. (2015). Locally welded silver nano‐network transparent electrodes with high operational stability by a simple alcohol‐based chemical approach. Advanced Functional Materials, 25(27), 4211-4218.

[27] Liu, Y., Zhang, J., Gao, H., Wang, Y., Liu, Q., Huang, S., ... & Ren, Z. (2017). Capillary-force-induced cold welding in silver-nanowire-based flexible transparent electrodes. Nano letters, 17(2), 1090-1096.

[28] Tas, N., Sonnenberg, T., Jansen, H., Legtenberg, R., & Elwenspoek, M. (1996). Stiction in surface micromachining. Journal of Micromechanics and Microengineering, 6(4), 385.

[29] Tsoukalas, K., Lahijani, B. V., & Stobbe, S. (2020). Impact of transduction scaling laws on nanoelectromechanical systems. Physical Review Letters, 124(22), 223902.

[30] Zou, J., Marcet, Z., Rodriguez, A. W., Reid, M. T. H., Mccauley, A. P., Kravchenko, I. I., ... & Chan, H. B. (2013). Casimir forces on a silicon micromechanical chip. Nature communications, 4(1), 1-6.

[31] Tang, L., Wang, M., Ng, C. Y., Nikolic, M., Chan, C. T., Rodriguez, A. W., & Chan, H. B. (2017). Measurement of non-monotonic Casimir forces between silicon nanostructures. Nature Photonics, 11(2), 97-101.

[32] Fong, K. Y., Li, H. K., Zhao, R., Yang, S., Wang, Y., & Zhang, X. (2019). Phonon heat transfer across a vacuum through quantum fluctuations. Nature, 576(7786), 243-247.